Journal of Biotechnology 202 (2015) 78–87

Contents lists available at ScienceDirect

Journal of Biotechnology

journal homepage: www.elsevier.com/locate/jbiotec

N-glycoprofiling analysis in a simple glycoprotein model: A comparison between recombinant and pituitary glycosylated human prolactin

Marcos V.N. Capone, Miriam F. Suzuki, João E. Oliveira, Renata Damiani, Carlos R.J. Soares*, Paolo Bartolini

Biotechnology Center, Instituto de Pesquisas Energéticas e Nucleares, IPEN – CNEN/SP, 05508-000 São Paulo, Brazil

ARTICLE INFO

Article history:
Received 3 July 2014
Received in revised form 7 November 2014
Accepted 20 November 2014
Available online 10 December 2014

Keywords:
N-glycoprofiling
Prolactin
Glycosylated human prolactin
G-hPRL
Cycloheximide

ABSTRACT

Human prolactin (hPRL) is a polypeptide hormone occurring in the non-glycosylated (NG-hPRL) and glycosylated (G-hPRL) forms, with MM of approximately 23 and 25 kDa, respectively. It has a single, partially occupied N-glycosylation site located at Asn-31, which makes it a particularly simple and interesting model for glycosylation studies. The bioactivity of G-hPRL is lower than that of NG-hPRL (by ca. 4-fold) and its physiological function is not clear. However, carbohydrate moieties generally play important roles in the biosynthesis, secretion, biological activity, and plasma survival of glycohormones and can vary depending on the host cell. The main objective of this study was to determine the N-glycan structures present in native, pituitary G-hPRL and compare them with those present in the recombinant hormone. To obtain recombinant G-hPRL, genetically modified Chinese hamster ovary cells (CHO), adapted to growth in suspension, were treated with cycloheximide, thus increasing the glycosylation site occupancy from 5.5% to 38.3%, thereby facilitating G-hPRL purification. CHO cell-derived G-hPRL (CHO-G-hPRL) was compared to pituitary G-hPRL (pit-G-hPRL) especially with regard to N-glycoprofiling. Among the main differences found in the pituitary sample were an extremely low presence of sialylated (1.7%) and a high percentage of sulfated (74.0%) and of fucosylated (90.5%) glycans. A ~6-fold lower in vitro bioactivity and a higher clearance rate in mice were also found for pit-G-hPRL versus CHO-G-hPRL. N-Glycan profiling proved to be a useful and accurate methodology also for MM and carbohydrate content determination for the two G-hPRL preparations, in good agreement with the values obtained directly via MALDI-TOF-MS.

1. Introduction

Human prolactin (hPRL) is a pituitary-secreted polypeptide hormone whose essential role is on mammopoiesis. In addition, it exerts many other physiological actions on behavior and brain in general and on metabolism, immune responses and electrolyte balance (Bernichtein et al., 2010; Goffin et al., 2002). Several experimental studies have defined this hormone as the "regulator of maternal behavior", but recent studies also consider it to be a candidate "regulator of paternal behavior" (Gettler et al., 2012). The interest in hPRL stems from its clinical importance for women with lactation problems and infertility, as well as from the fact that elevated circulating levels or locally produced hPRL are associated with increased risks of breast and prostate cancer (Bernichtein et al., 2010; Fernandez et al., 2010; Suzuki et al., 2012; Tworoger et al., 2004).

Human prolactin (hPRL) is a 199 amino acid-polypeptide with a single potential N-glycosylation site located at Asn-31, which is partially (5–30%) occupied in the native pituitary form or in the recombinant form of the hormone (Heller et al., 2010; Price et al., 1995; Sinha, 1995; Soares et al., 2000, 2002). It thus exhibits the

Abbreviations: CDG, congenital disorders of glycosylation; CHO, Chinese hamster ovary; CHX, cycloheximide; hPRL, human prolactin; HPSEC, size-exclusion HPLC; MALDI-TOF-MS, matrix assisted laser desorption ionization time-of-flight mass spectrometry; MM, molecular mass; Mr, relative molecular mass; NHPP, National Hormone and Pituitary Program; PAGE, polyacrylamide-gel electrophoresis; SDS, sodium dodecyl sulfate; RP-HPLC, reverse-phase HPLC; t_R, retention time.

* Corresponding author at: Instituto de Pesquisas Energéticas e Nucleares, IPEN – CNEN/SP, Biotechnology Center, Av. Prof. Lineu Prestes 2242, São Paulo, SP 05580-000, Brazil. Tel.: +55 11 3133 9693; fax: +55 11 3133 9694.
E-mail address: crsoares@ipen.br (C.R.J. Soares).

http://dx.doi.org/10.1016/j.jbiotec.2014.11.034
0168-1656/

simplest type of glycosylation macroheterogeneity: one protein population with and one without a single N-linked glycan (Heller et al., 2010; Shelikoff et al., 1994). This makes it particularly ideal for glycosylation studies, especially considering the complexity of glycan composition and the challenging task of the simultaneous accurate determination of: (i) protein concentration; (ii) oligosaccharide structures (i.e., the variation of the glycoform profile); and (iii) the glycosylation site occupancy of glycoproteins in general (Apweiler et al., 1999; Desaire, 2013; Lin et al., 2012; Pan et al., 2012; Petrescu et al., 2004).

Glycosylated hPRL (G-hPRL) has an approximately 4-fold lower potency compared to the non-glycosylated form (NG-hPRL), showing reduced lactotrophic and mitogenic activity (Heller et al., 2010; Price et al., 1995; Shelikoff et al., 1994; Sinha, 1995). Although it has been considered to be the major post-translational modification of NG-hPRL, with which it is co-secreted from childhood to the end of puberty, its physiological significance is still not yet well elucidated (Fideleff et al., 2012; Freeman et al., 2000).

Because it is such a simple monoglycosylation model, G-hPRL has been chosen to develop a methodology for determining oligosaccharide structures and glycosylation site occupancy via glycoprofiling analysis. After it has been validated, this methodology should then be applicable also to more complex polyglycosylated proteins. The importance of correctly knowing these parameters has been emphasized in the literature. Thus, comparative quantitative profiling of a glycoproteome and the accurate quantification of its glycosylation site occupancy have been related to folding, trafficking, initiation of inflammation, and host defense, as well as to disease states such as congenital disorders of glycosylation (CDG). These latter are a family of rare, inherited metabolic syndromes that affect the synthesis, transfer or processing of glycans and that cause motor and intellectual disability and variable multisystemic symptoms. In type-I CDG the early steps of glycosylation are impaired, resulting in unoccupied glycosylation sites; in type-II CDG the defects do not influence occupancy, but rather glycan processing (Barone et al., 2009; Fogli et al., 2012; Losfeld et al., 2012; Pan et al., 2012; Petrescu et al., 2004; Tian and Zhang, 2010).

The present study is based on suspension-adapted prolactin-secreting CHO cells, cultivated in spinner flasks and incubated in the presence of cycloheximide in order to increase the proportion of G-hPRL in the total amount of prolactin and facilitate its purification. Purified G-hPRL, which is now a 100% occupied monoglycosylated protein, is then extensively characterized by SDS-PAGE, Western blotting, reverse-phase and size-exclusion HPLC, in vitro bioassay, pharmacokinetic analysis, MALDI-TOF-MS relative molecular mass (Mr) determination and, finally, N-glycan[1] profiling. Our recombinant preparation (CHO cell-derived) is compared to the native pituitary (lactotrophic cell-derived) preparation, using a well-known reference from the National Hormone and Pituitary Program (NHPP, USA). Accurate MALDI-TOF-MS molecular mass determination was employed to confirm that the glycoprofiling approach is indeed useful for correctly determining, besides the monosaccharide composition of each glycan, also the average glycan mass, the whole glycoprotein mass and, consequently, the percent molecular weight exclusively due to the carbohydrate moiety in the two preparations.

[1] Abbreviations for N-glycans were made by not considering the basic pentasaccharidic nucleus ("zero") and adding all other monosaccharides, as stated in the figures, in the following order: Man (**M**); GlcNAc (**N**); Gal (**G**); GalNAc (**Gn**); NeuAc/sialic acid (**S**); Fuc (**F**). So, for example, $NeuAc_1$ Gal_1 $GlcNAc_2$ $Fuc_1 + Man_3$ $GlcNAc_2$, becomes **N2G1S1F1**.

2. Materials and methods

2.1. Cell line

The clone expressing hPRL, obtained in our laboratory and utilized in this study, was derived from CHO dhfr-cells (DUKX-B11) that had been transfected with the vector pEDdc-hPRL (Soares et al., 2000) and adapted to suspension growth in serum-free medium (Arthuso et al., 2012).

2.2. G-hPRL production in spinners

For laboratory production, 250 ml spinner flasks containing 100 ml of CHO-S-SFM II medium, supplemented with antibiotics (50 unit ml^{-1} penicillin; 50 $\mu g\,ml^{-1}$ streptomycin, 40 $\mu g\,ml^{-1}$ gentamycin and 1.25 $\mu g\,ml^{-1}$ amphotericin B), were utilized. Cells were cultured at 37 °C under 5% CO_2, stirring at ~80 rpm. When a density of 1×10^6 cell ml^{-1} was obtained, the total volume of conditioned medium (100 ml) was centrifuged at 400 × *g* and substituted with fresh medium, with the initial cell concentration fixed at $\sim 1 \times 10^6$ cell ml^{-1}. In this phase, CHX (0–1 $\mu g\,ml^{-1}$, depending on the experiment) was added and the conditioned medium, collected daily by centrifugation at 400 × *g*, was replaced with a fresh one. This procedure was repeated for 10 days. The collected medium was stored at −40 °C.

2.3. Gel electrophoresis and Western blotting

Discontinuous SDS-PAGE, based on 15% polyacrylamide gels, was carried out under non-reducing conditions as described by Laemmli (1970). Coomassie Brilliant Blue G-250 (USB, Cleveland, OH) or silver nitrate was used for staining; the molecular mass markers were from GE Healthcare Bio-Sciences (Uppsala, Sweden).

For the Western blotting the proteins were transferred from the polyacrylamide gel to nitrocellulose membrane by the semi-dry transfer technique, probed with polyclonal anti-hPRL antiserum produced in rabbit (1:5000) and with horseradish peroxidase-conjugated anti-rabbit IgG (1:10,000). Visualization of proteins was performed with Luminata Forte (Millipore) on X-ray film.

2.4. HPSEC

A Shimadzu Model SCL-10A HPLC apparatus coupled to a SPD-10AV UV detector (Shimadzu, MD, USA) was used, employing the Class VP software, also from Shimadzu. For HPSEC, a TosoHaas (Montgomeryville, PA, USA) G2000 SW column (60 cm × 7.5 mm i.d., particle size of 10 μm and pore size of 125 Å) coupled to a 7.5 cm × 7.5 mm ID SW guard column was used. The mobile phase was 0.025 M ammonium bicarbonate, pH 7.0, with a flow-rate of 1.0 ml min^{-1} (Dalmora et al., 1997).

2.5. G-hPRL purification

The G-hPRL present in the conditioned culture medium was purified using a two-step purification method: SP-Sepharose Fast Flow followed by a C4 Grace-Vydac 214TP54 (25 cm × 4.6 mm ID, pore diameter of 300 Å and particle diameter of 5 μm) RP-HPLC column, used for preparative purposes. Briefly, conditioned medium (2000 ml) was adjusted to pH 5.0 using acetic acid. The material was then applied (5 ml min^{-1}) onto a 10 cm × 2.6 cm ID glass column packed with SP-Sepharose Fast Flow (GE Healthcare Bio-Sciences AB, Uppsala, Sweden) that had been previously equilibrated in 50 mM sodium acetate (pH 5.0). UV absorbance was monitored at 280 nm. After washing with the same buffer, the column was eluted with 50 mM sodium acetate (pH 5.0), 90 mM NaCl. Human PRL (G-hPRL and NG-hPRL) was then eluted from the column with 25 mM

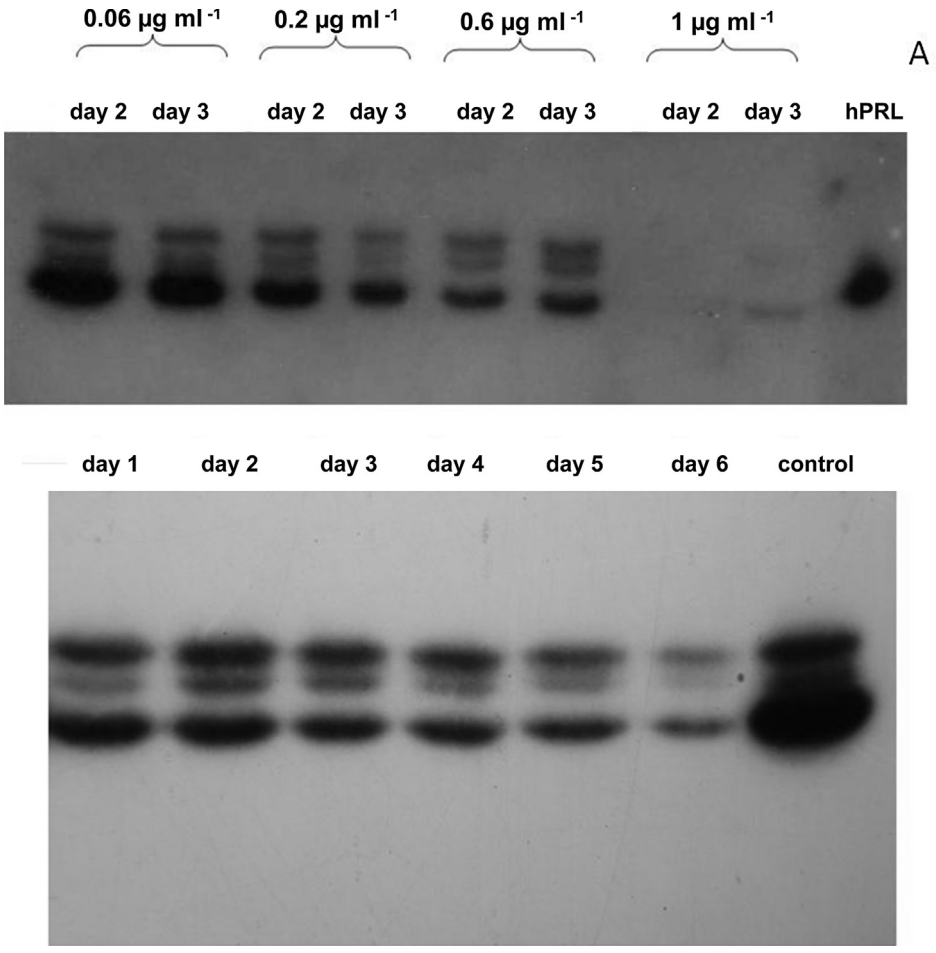

Fig. 1. Western blot analysis of hPRL from CHO cells conditioned media obtained in spinner flasks. (A) Samples obtained on the 2nd and 3rd day of production in the presence of different concentrations of cycloheximide; hPRL, internal reference preparation of *E. coli*-derived hPRL. (B) Samples obtained during a 6-day production cycle in the presence of 0.6 µg ml^{-1} of cycloheximide; control, product obtained without cycloheximide addition.

Hepes (pH 8.0). All fractions containing hPRL were analyzed by SDS-PAGE and the most concentrated fractions pooled and loaded onto a Grace-Vydac C4 214 TP54 RP-HPLC column, equilibrated in 0.05 M sodium phosphate buffer containing 45% acetonitrile. The maximum volume applied for each RP-HPLC preparative run was 6 ml (3× 2 ml applied sequentially). A washing step with the same buffer, carried out over 60 min, was followed by the elution of G-hPRL with 50% acetonitrile, pH 7.0, at a flow rate of 0.5 mL min^{-1} for 30 min at 30 °C. A G-hPRL final pool, derived from RP-HPLC purification, was analyzed by SDS-PAGE and HPSEC and stored at −80 °C, before lyophilization, for N-glycan structure analysis (glycoprofiling).

2.6. In vitro bioassays

The biological activities of purified G-hPRL were determined by the Nb2 lymphoma cell-proliferation assays, as previously described (Glezer et al., 2006), against the First WHO Reference Reagent of recombinant hPRL lyophilized in ampoules coded 97/714. This preparation includes NG-hPRL and G-hPRL and its biological activity (57.2 IU mg^{-1}) was established thanks to a WHO-NIBSC International Collaborative Study, also carried out with participation of our laboratory (Rafferty et al., 2001). The curves were constructed after subtraction of the medium control.

2.7. Pharmacokinetic analysis

Single doses (2 µg) of the different G-hPRL preparations were administered to BALB/c mice (three animals per group) by intraperitoneal injection. Blood was withdrawn from the retro-orbital cavity at 30, 60, 90, 120 and 180 min post injection and serum samples were obtained by incubating 20 min at 37 °C, then 20 min at 4 °C and centrifuging 7 min at 2500 × *g*. Serum G-hPRL concentrations were determined using a human PRL double antibody ELISA kit (Diagnostic Systems, Ltd., Novogorod, Russia). No cross-reaction was detected with endogenous mouse-PRL and its response to G-hPRL was about 40% less than that to NG-hPRL.

2.8. Mass spectrometry for molecular mass determination

MALDI-TOF-MS molecular mass determinations of hPRL (NG-hPRL and G-hPRL) were carried out by American International Biotechnology (AIBio Tech) Services, (Richmond, VA, USA) using sinapinic acid (SA) as the matrix and a Voyager-DE BioSpectrometry Workstation from Applied Biosystems (Foster City, CA, USA).

2.9. N-glycosylation profiling by MALDI-TOF-MS

The analysis of the N-glycan structures was carried out by Proteodynamics SARL (Clermont-Ferrand, France). Two samples were analyzed: recombinant G-hPRL IPEN produced in our laboratory and a pituitary G-hPRL obtained from Dr. A.F. Parlow of the National Hormone and Peptide Program (NHPP) (Torrance, CA, USA), both lyophilized.

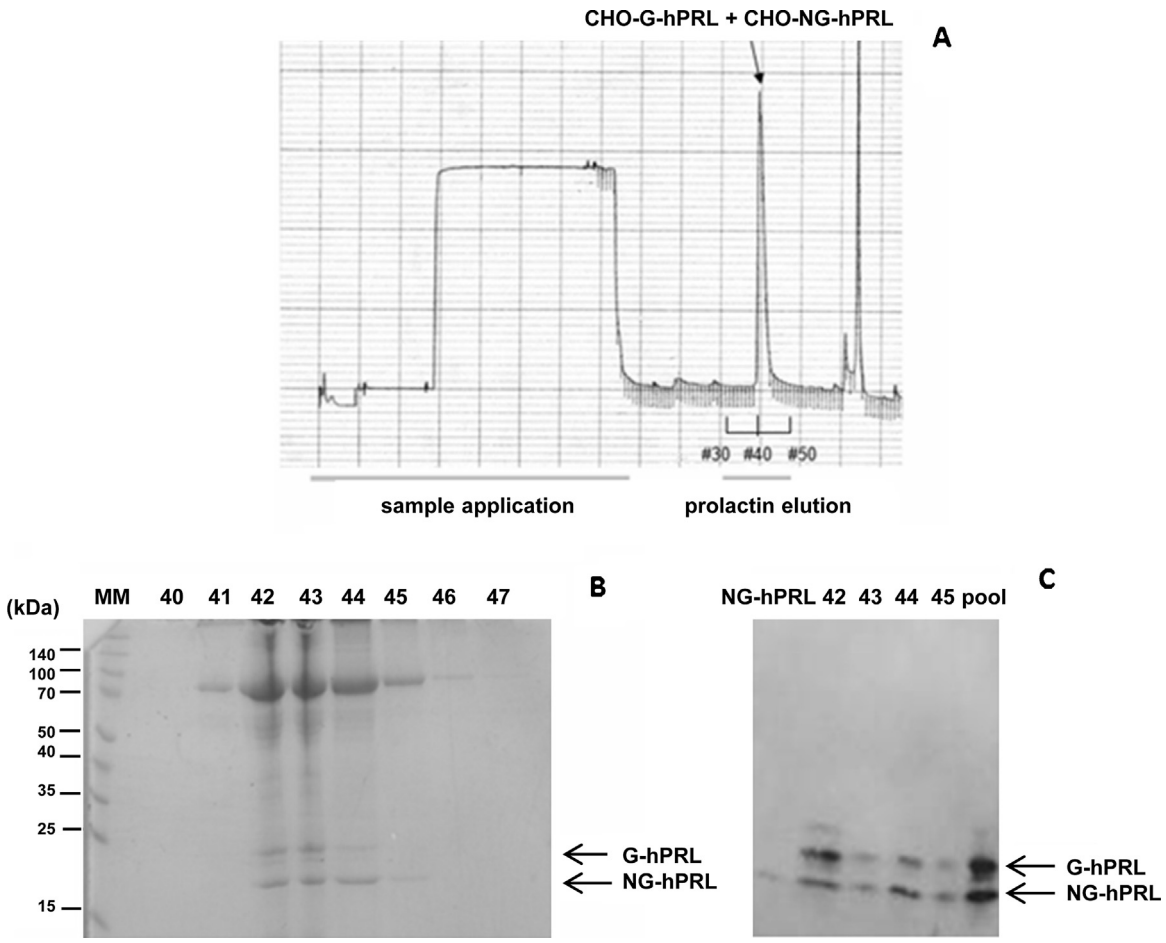

Fig. 2. (A) SP-Sepharose FF purification of hPRL from 1 l of CHO cell culture medium obtained in the presence of 0.6 μg ml^{-1} of cycloheximide. (B) SDS-PAGE analysis of different fractions of the main peak (#40–47) corresponding to CHO-G-hPRL + CHO-NG-hPRL, based on 15% polyacrylamide gels under non-reducing conditions and stained with Coomassie Brilliant Blue G-250. MM, molecular mass markers. (C) Western blotting corresponding to fractions # 42–45 and to the pool of these fractions; NG-hPRL, *E. coli*-derived hPRL.

2.10. Glycosidase digestion and permethylation of N-glycans

Proteins (260 μg of CHO-derived G-hPRL and 340 μg of pituitary G-hPRL) were denatured in 0.5% sodium dodecyl sulphate (SDS) and 1% β-mercaptoethanol (90 °C, 10 min) and deglycosylated by enzymatic digestion treating for 15 h at 37 °C with 20 units PNGase F (lot 13643021) from Roche Applied Science (Mannheim, Germany), according to Fogli et al. (2012). Deglycosylation was monitored on a NuPage gradient of 4–12% MES (Invitrogen) by Coomassie blue staining.

A specifically adapted permethylation protocol based on Yu et al. (2009) was employed to separate sulfated from non-sulfated or phosphorylated N-glycans of pituitary G-hPRL. After permethylation, the N-glycans were purified on C18 Sep Pak Plus (Waters, Milford, MA) by step-elution with 25% acetonitrile and 50% acetonitrile. The 25% acetonitrile fraction contains sulfated glycans, present only in the pituitary product, while non-sulfated and phosphorylated glycans are found in the 50% acetonitrile fraction. Eluted N-glycans were lyophilized before MALDI-TOF-MS analysis.

2.11. MALDI-TOF analysis of N-glycans

Mass spectra of permethylated N-glycans resuspended in 20 μl of 50% methanol/water were acquired in the positive reflector mode (m/z range 1000–5000 Da) on MALDI-TOF DE PRO (ABsiex, Inc., Framingham, MA) with DHB as matrix (10 mg ml^{-1}, ratio 1:1).

The spectra were obtained by accumulation of 500 shots and were calibrated with an external standard. MALDI-MS data were processed using DataExplorer 4.0 to generate files listing m/z values and to compare intensities. Interpretation of glycan structures corresponding to monoisotopic masses was performed using EXPAZY GlycoMod tool (http://ca.expasy.org/tools/glycomod/) and GlycoWorkBench. MALDI-PSD fragmentation was performed on selected ions to confirm structures.

To obtain a relative quantification comprising all N-glycans present on the pituitary-derived protein, a correlation factor between the spectra of sulfated and native glycans was calculated. This correlation factor was determined either by using an internal calibration standard to normalize peak intensities of the two spectra or by mixing the two glycan fractions and using the ratio between peak heights of the dominant peaks of each fraction.

2.12. Monosaccharide molar ratio determination on the basis of glycoprofiling

The glycoprofiling and the relative percent intensity of each determined glycan were used to calculate the average N-glycan mass that is present in the G-hPRL molecule. This mass, added to the theoretical molecular mass of NG-hPRL (22,897.75 Da), provided a good estimate of the G-hPRL molecular mass and of the percent by weight of the carbohydrate moiety. Through this stoichiometric approach, the percentage of each monosaccharide and its molar ratio, referred to the G-hPRL molecule, were also calculated (see Supplementary Material).

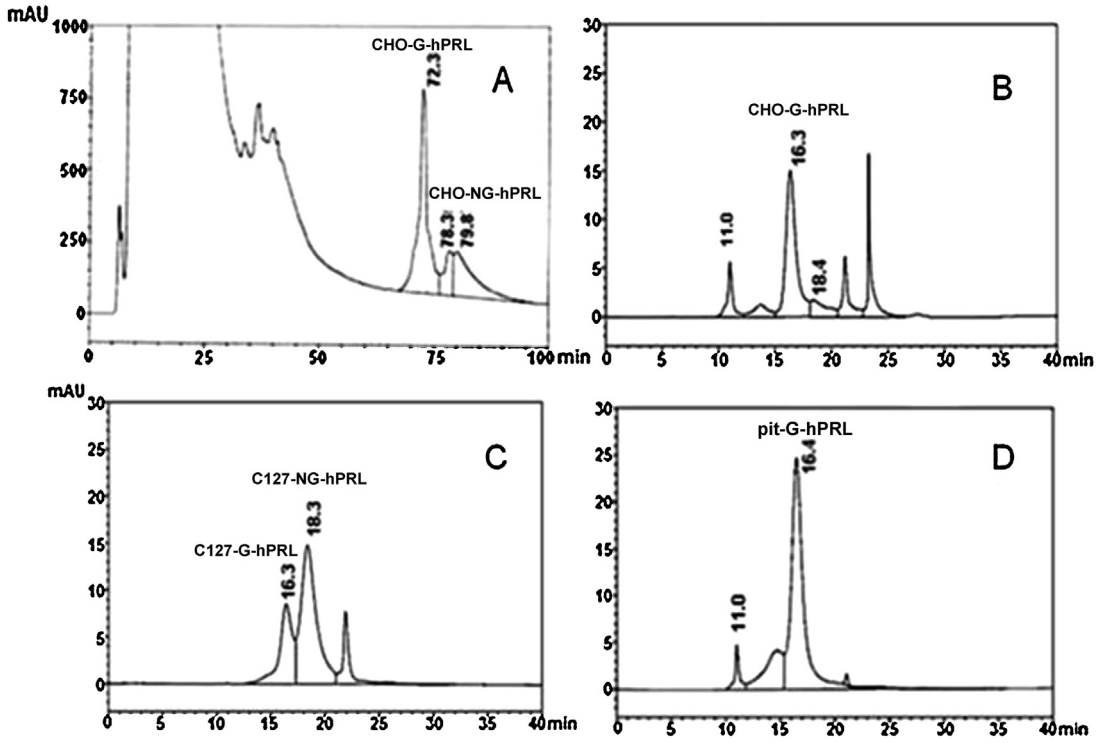

Fig. 3. Second purification step of CHO-G-hPRL. (A) RP-HPLC (25 cm × 4.6 mm ID column) used in the preparative mode: 3 × 2 ml from the main SP-Sepharose peak were applied in each run. HPSEC analysis of: (B) the main peak eluted from RP-HPLC; (C) CRS–WHO containing C127-G-hPRL + C127-NG-hPRL; and (D) pit-G-hPRL from NHPP.

3. Results and discussion

3.1. Prolactin synthesis inhibition and purification

Considering previous work reporting the effects of cycloheximide on hPRL-secreting, adherent CHO cell culture (Heller et al., 2010) the effects of this drug were investigated under the present culture conditions: suspension-adapted cells, spinner flask culture and serum-free medium, as described by Arthuso et al. (2012). The optimal cycloheximide concentration to be added to the culture medium in order to obtain the highest glycosylation site occupancy was determined by Western blotting, as shown in Fig. 1A. The increase in cycloheximide concentration produced a remarkable reduction in the amount of NG-hPRL, while G-hPRL remained practically the same. With 1 μg ml^{-1} cycloheximide, however, both isoforms declined dramatically. The concentration of 0.6 μg ml^{-1} was thus chosen for G-hPRL synthesis, in line with that adopted by Heller et al. (2010). This condition was also used for the 6-day production cycle illustrated in Fig. 1B, which shows that the drug was already fully effective on day 1. A third, weaker band was also observed in this experiment: probably a glycosylated isoform.

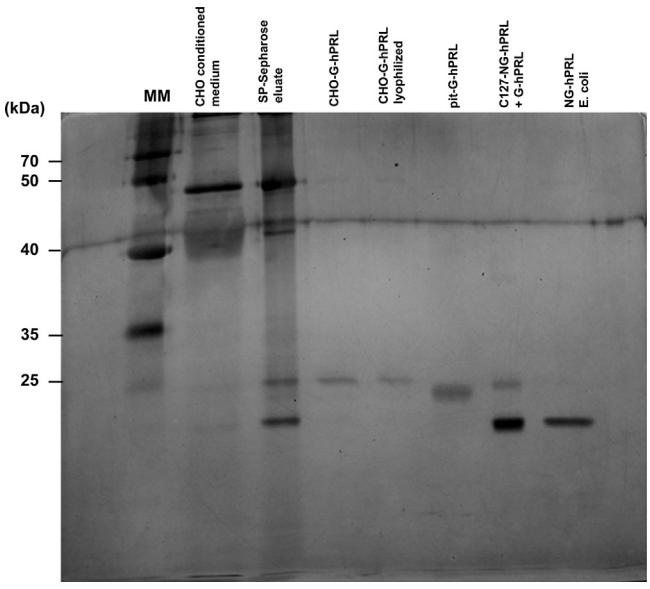

Fig. 4. SDS-PAGE analysis under non-reducing conditions and stained with silver nitrate, of all purification steps of CHO-G-hPRL. (1) Molecular mass markers; (2) 10-day production conditioned medium; (3) main peak eluted from SP-Sepharose; (4) pure CHO-G-hPRL obtained after RP-HPLC elution; (5) purified CHO-G-hPRL after lyophilization; (6) pit-G-hPRL from NHPP; (7) CRS-WHO containing C127-G-hPRL + C127-NG-hPRL; and (8) internal reference preparation of *E. coli*-NG-hPRL.

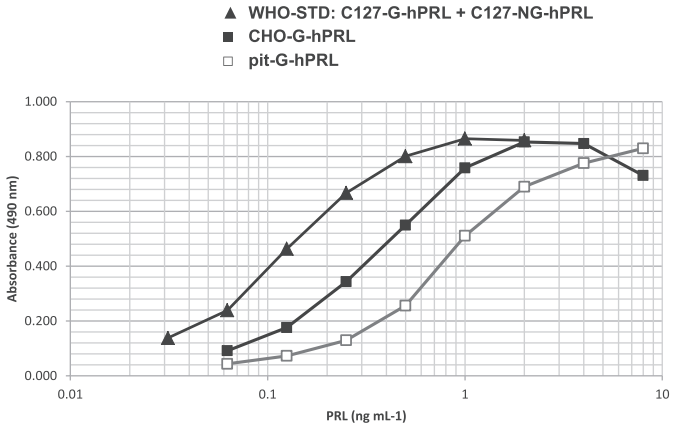

Fig. 5. Nb2 cell proliferation bioassay comparing the biological activities of purified CHO-G-hPRL (-■-) and pit-G-hPRL from NHPP (-□-) with the International Standard of C127-derived hPRL WHO 97/714, containing C127-G-hPRL + C127-NG-hPRL (-▲-).

Table 1
Pharmacokinetic parameters for CHO-derived and pituitary G-hPRL.

Preparation	$t_{1/2}$ (min)	AUC (ng min ml^{-1})
CHO-derived G-hPRL	36.0	6279.5
Pituitary G-hPRL	34.5	2615.5

To evaluate cycloheximide effects on cell growth and viability, two spinner flasks, with or without cycloheximide addition, were compared in a 10-day production cycle, replacing the culture medium daily, as in a regular production scheme. A small decrease (~6%) in cell concentration was observed upon cycloheximide addition, confirming that the concentration chosen was only slightly toxic to the cells (data not shown).

The purification process of recombinant G-hPRL consisted of two steps: an initial concentration/purification step carried out by cation exchange chromatography on SP-Sepharose FF and a second step based on a small analytical RP-HPLC column, used in the preparative mode. The cation exchanger provided a main peak containing both NG-hPRL and G-hPRL (Fig. 2A), as confirmed by SDS-PAGE analysis (Fig. 2B). Western blotting, moreover, confirmed that the high MM material observed in SDS-PAGE is not related to prolactin (Fig. 2C). Qualitative and quantitative RP-HPLC analysis carried out after this step showed the expected marked decrease (~16-fold) of NG-hPRL (from 3088 ± 80 to 190 ± 55 μg ml^{-1}, n = 3) upon cycloheximide addition, while G-hPRL decreased only ~30% (from 178 ± 75 to 118 ± 52 μg ml^{-1}, n = 3). The reduction in elongation rate provoked by cycloheximide addition thus increased the N-glycosylation site occupancy from 5.5% to 38.3%. Preparative RP-HPLC, carried out as in previous work for mouse prolactin purification (Suzuki et al., 2012), had the advantage of using a small column (25 cm × 4.6 mm i.d.) to process a relatively large volume (about 20 ml) of the SP-Sepharose eluted peak in only three runs, obtaining a separation between CHO-G-hPRL and CHO-NG-hPRL (Fig. 3A).

3.2. Characterization of CHO-derived G-hPRL

In a relatively short time preparative RP-HPLC provided a >90% pure product. This is shown in analytical HPSEC (Fig. 3B) in which the retention time (t_R) of the main peak of G-hPRL is well preserved compared with the CRS (C127-derived chemical research standard – WHO) containing C127-G-hPRL + C127-NG-hPRL (Fig. 3C) and with human pituitary G-hPRL (Fig. 3D), with only minor peaks due to buffer components (t_R > 20 min) and probably a small amount of aggregate (t_R = 11 min).

Silver stained SDS-PAGE (Fig. 4) was employed to confirm the purity of G-hPRL IPEN obtained via this process, together with the analysis of all intermediate steps. Although it is almost impossible to detect the two PRL isoforms in the conditioned medium (lane 2), they can be very clearly seen in the SP-Sepharose eluted peak (lane 3). A band of RP-HPLC-purified G-hPRL is then visible in lane 4 and in the final lyophilized product (lane 5), again with a very small amount of the faster-running band mentioned above. Interestingly, the band of pituitary G-hPRL with an apparent lower molecular mass can be observed in lane 6 and, in lane 7, C127-G-hPRL from WHO-CRS with an intermediate mass. Finally, lane 8 confirms the constant position of NG-PRL.

The biological activity of CHO-G-hPRL, determined by the Nb2 cell in vitro bioassay, was 20.4 ± 1.7 IU mg^{-1} (n = 2), i.e., ~3-fold lower than that defined for NG-hPRL 63.7 IU mg^{-1} (Rafferty et al., 2001). This confirms literature values, including that reported by Heller et al. (2010) for a similar CHO cell-derived G-hPRL preparation (14.7 ± 5.7 IU mg^{-1}). The potency of pit-G-hPRL from NHPP, on the other hand, was 3.6 ± 0.2 IU mg^{-1}, i.e. 5.7-fold lower than that of CHO-G-hPRL. Typical Nb2 assay curves, including that of the International Standard of Recombinant hPRL (WHO 97/714) used for potency determination, are shown in Fig. 5. It is important to note, however, that the Nb2 proliferative assay, even being the most widely used for human prolactin bioactivity determination, only measures a particular type of activity. It would be interesting to determine and compare, for both preparations, G-hPRL activity related to other physiological actions such as, for example, milk protein induction or salt reuptake in the kidney. Quite intriguing is also the fact that pit-G-hPRL shows an ~6-fold lower bioactivity than CHO-G-hPRL. We do not have a ready explanation for this, unless we think of the possible influence of the different carbohydrate moiety at the receptor level. We found, in previous work, differences of the same order (up to 3.4–4.2-fold) when comparing pituitary with CHO-derived hTSH (Damiani et al., 2013). In that case, however, an in vivo bioassay was utilized and there was certainly an influence on the clearance rate due to the presence of terminal GalNAc-4-SO4 and β1,4-linked GalNAc in the pituitary preparation.

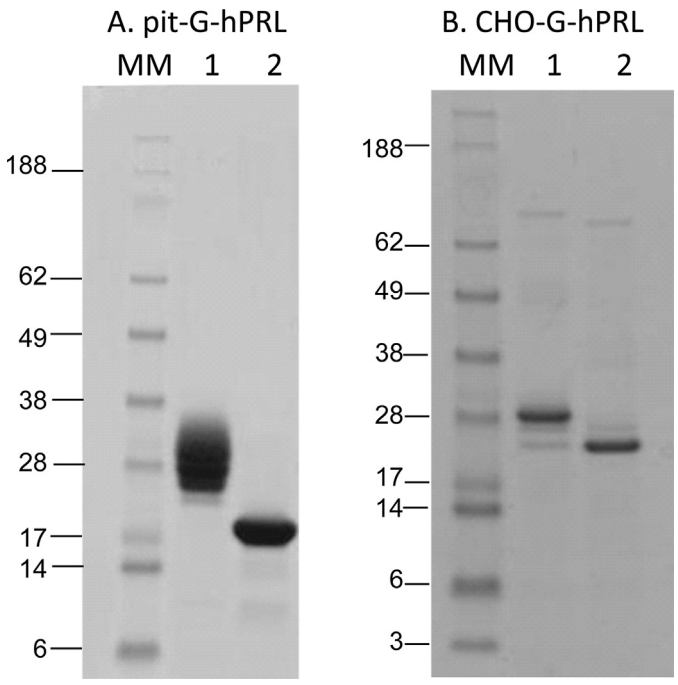

Fig. 6. NuPAGE gradient electrophoresis under reducing conditions and stained with Coomassie Brilliant Blue, showing the deglycosylation of: (A) pit-G-hPRL from NHPP and (B) CHO-G-hPRL. Lane 1, G-hPRL; lane 2, G-hPRL treated with peptide-N-glycosidase F (PNGase F).

A preliminary pharmacokinetic study was carried out by comparing the in vivo clearance rate of CHO-derived and pituitary G-hPRL in normal mice. Table 1 shows that there is a tendency to an increased half-life ($t_{1/2}$) and area-under-the curve (AUC) for the recombinant preparation. Confirming our previous data on analogous hTSH preparations (Damiani et al., 2013), the shorter circulatory half-life of pituitary G-hPRL is probably due, among other factors, to the presence of the terminal sequence GalNAc-4-SO_4 that determines a removal of G-hPRL from the circulation by a specific receptor expressed by endothelial cells lining the sinusoids of the liver (Baenziger, 2003; Mi et al., 2008). The presence, however, of 74% sulfated N-glycans in pit-G-hPRL should have determined, in our opinion, a much higher clearance rate.

3.3. N-glycoprofiling of pituitary and recombinant G-hPRL

Our CHO cell-derived G-hPRL was then compared with native pituitary G-hPRL with respect to the N-glycan structures. The

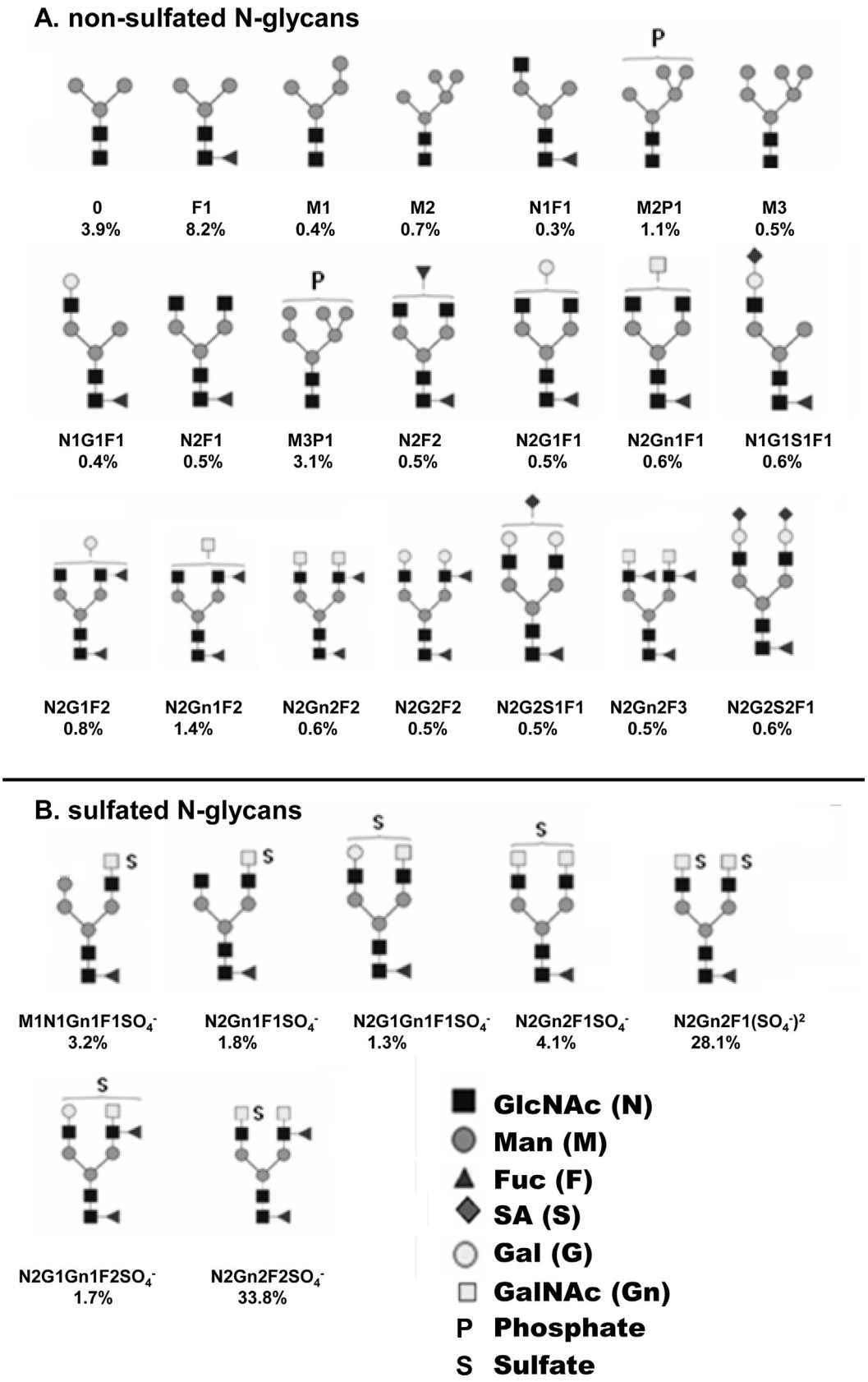

Fig. 7. N-glycan structures of pit-G-hPRL from NHPP. (A) Non-sulfated N-glycans; (B) sulfated N-glycans. The relative percent intensity is indicated below each glycan structure. See the text for N-glycan nomenclature.

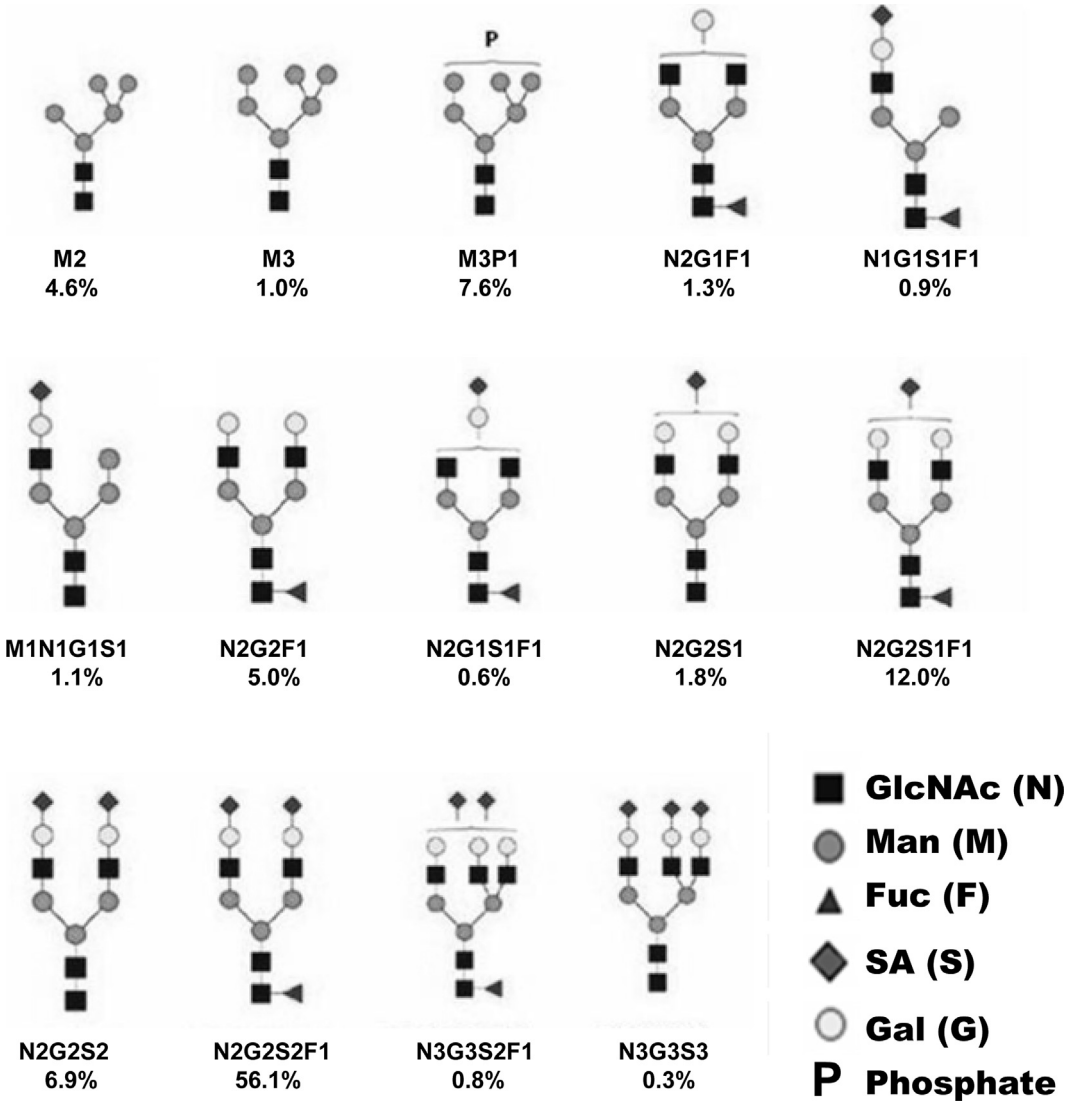

Fig. 8. N-glycan structures of CHO-G-hPRL. The relative percent intensity is indicated below each glycan structure. See "Abbreviations" for N-glycan nomenclature.

occupancy, now 100%, was re-confirmed via NuPAGE gradient electrophoresis after glycosidase digestion, as shown in Fig. 6 for the native and recombinant preparations. In the native preparation, the larger, more heterogeneous G-hPRL band was totally converted into a narrower band of NG-hPRL by deglycosylation. In the case of the recombinant preparation, however, a small amount of NG-hPRL appears as a contaminant, even before deglycosylation (Fig. 6B). Figs. 7 and 8 show the N-glycosylation profiling and relative intensities obtained by MALDI-TOF-MS after glycosidase digestion and N-glycan permethylation of native and CHO-cell-derived G-hPRL, respectively. The quantitative monosaccharide determination for both preparations and the corresponding molar ratios derived from N-glycoprofiling shown in Table 2 are based on a stoichiometric calculation which considered the molecular mass and relative intensities of each detected N-glycan, as described in Section 2. The average glycan mass, also calculated on the basis of the same parameters, was 2118.0 Da for CHO cell-derived and 1837.8 Da for lactotroph cell-derived G-hPRL (Table 3). See also the Supplementary Material on "Mass spectral Data".

In native G-hPRL (Fig. 7 and Table 2), some high-mannose (~6%), mostly complex structures, frequently fucosylated (90.5%) and rarely sialylated (1.7%), are present. As expected, since human lactotroph cells have galactosyl- and sulpho-transferases that are absent in CHO cells, the glycans of the former have a high percentage of sulfated glycans (74%) and a significant amount of N-acetyl galactosamine (GalNAc), sulphated or not: 1.31 mole mole^{-1}. The amount of galactose is quite low (0.081 mole mole^{-1}) and that of sialic acid extremely low (0.02 mole mole^{-1}). The most abundant N-glycans are of the biantennary type: $N2Gn2F2SO_4$ (33.8%) and $N2Gn2F1(SO_4)_2$ (28.1%).

CHO cell-derived G-hPRL (Fig. 8 and Table 2) has a higher percentage of high-mannose forms (~13%), mostly complex structures, obviously no GalNAc or sulfated glycans, and much higher amounts of galactose (1.62 mole mole^{-1}) and sialic acid (1.34 mole mole^{-1}). The most abundant N-glycans are also of the biantennary type: N2G2S2F1 (56%) and N2G2S1F1 (12%). There is also a small presence (1.1%) of triantennary structures, not found in the native product. Preliminary data on N-glycoprofiling for CHO-derived G-hPRL IPEN obtained without cycloheximide, confirmed a similar distribution for the most abundant N-glycan forms, with a relatively higher presence of galactose (1.95 mole mole^{-1}) and sialic acid (1.74 mole mole^{-1}), all other parameters being practically unaltered.

Post source decay (PSD) fragmentation analysis of selected N-glycans, as for example of the two most abundant sulfated glycans presented in Fig. 7B (see Supplementary Material), was also

Table 2
Monosaccharide/G-hPRL molar ratio determination with basis on glycoprofiling.

	CHO cell-derived G-hPRL[a]			Native pituitary G-hPRL[b]		
	Fraction of glycan mass (%)	Monosaccharide weight contribution (Da)	Mole/G-hPRL mole	Fraction of glycan mass (%)	Monosaccharide weight contribution (Da)	Mole/G-hPRL mole
Fuc	5.03	106.5	0.73	10.10	185.6	1.27
Gal NAc	–	–	–	14.51	266.7	1.31
Glc NAc	35.70	756.1	3.72	39.94	734.0	3.61
Gal	12.42	263.1	1.62	0.720	13.2	0.081
Man	28.04	593.9	3.66	30.30	556.8	3.43
SA	18.38	389.3	1.34	0.323	5.94	0.020

[a] Considering the N-glycan mass = 2118.0 Da.
[b] Considering the N-glycan mass = 1837.8 Da.

Table 3
Molecular mass of CHO cell-derived, C127 cell-derived and native pituitary (lactotroph-derived) glycosylated prolactin, determined via N-glycoprofiling analysis and compared to MALDI-TOF-MS determinations.

Origin of the preparation	Via N-glycoprofiling			Via MALDI-TOF-MS			
	Average N-glycan mass (Da)	G-hPRL MM (Da)	Carbohydrate moiety (%)	NG-PRL (Mr)	G-PRL (Mr)	Carbohydrate moiety (%)	Difference between MM and Mr for G-hPRL (%)
CHO cells	2118.0	25016[a]	8.5[b]	22889[c]	24970[c]	8.3[e]	+0.18
C127 cells	–	–	–	22880[c]	25139[c]	9.0[e]	–
Human lactotrophs	1837.8	24736[a]	7.4[b]	22974[d]	24903[d]	7.7[e]	−0.67

[a] Calculated by adding the N-glycan mass to the calculated NG-hPRL mass of 22,897.75 (Wu et al., 2003).
[b] Calculated as a percent of the average glycan mass on G-hPRL MM.
[c] Data from Heller et al. (2010).
[d] Present work.
[e] Calculated on the basis of NG-hPRL and G-hPRL Mr.

carried out to further determine their structure, finding, though, no unusual ions. On the other hand the immunogenic Lewis X (Lex) motif GalGlcNAcFuc (Hashii et al., 2005; Lehr et al., 2006) was apparently present in the non-sulfated glycan N2G2F2 (Fig. 7A).

It is noteworthy that these are the first data on N-glycan structures that have been reported for G-PRL of either pituitary or recombinant origin. Price et al. (1995) inferred the monosaccharide composition of recombinant G-hPRL from oligosaccharide masses (range: 1972–2696) determined by electrospray ionization mass spectroscopy (ESI-MS), masses that are typical of biantennary and triantennary complex oligosaccharides with different degrees of sialylation and fucosylation. Despite using a product of different origin (CHO versus C127 cells), our more detailed analysis confirms their preliminary conclusion.

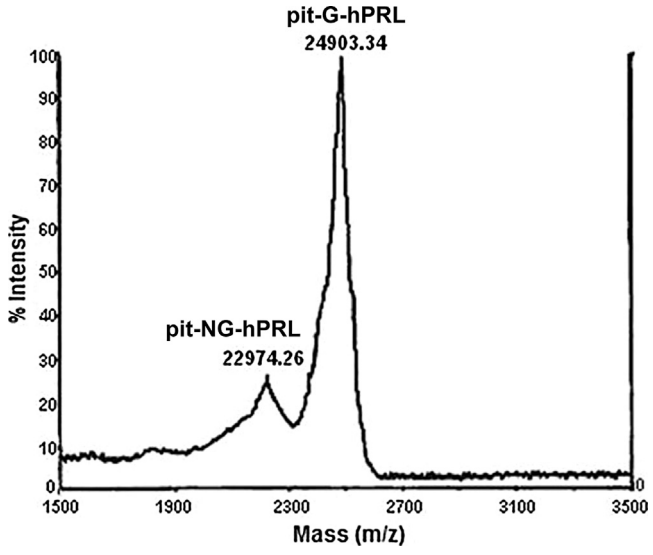

Fig. 9. MALDI-TOF-MS analysis of pit-G-hPRL from NHPP, including a certain amount of pit-NG-hPRL.

3.4. Molecular mass determination based on N-glycoprofiling and MALDI-TOF-MS analysis

In Fig. 9 we report the MALDI-TOF-MS determination carried out on native pituitary prolactin from NHPP, which shows the relative molecular mass (Mr) of G-hPRL and the presence of NG-hPRL as a contaminant. The exceptional accuracy and precision offered by this methodology is indicated by the present data on pituitary NG-hPRL and at least six previous determinations of the molecular mass of CHO-, C127- or *Escherichia coli*-derived NG-hPRL (Heller et al., 2010; Soares et al., 2006, 2008). The average inter-assay and inter-preparation molecular mass of this protein was 22,910.34 ± 32.22 (CV = 0.14%, $n = 6$), which is only 0.055% higher than the theoretical molecular mass of 22,897.75 Da calculated from the amino acid sequence (Wu et al., 2003) and 0.3% lower than the mass of pituitary NG-hPRL determined in the present work via MALDI-TOF-MS.

In Table 3 the molecular mass (MM) of both preparations of G-hPRL, determined on the basis of glycoprofiling and from the calculated theoretical mass of NG-hPRL, are reported in comparison with MALDI-TOF-MS Mr determinations for NG-hPRL and G-hPRL of different origins. There is good agreement between the two different analytical approaches for both the molecular mass and the percent carbohydrate.

4. Conclusions

CHO-derived human prolactin, a simple model of a monoglycosylated protein, was obtained with greatly increased glycosylation site occupancy via cycloheximide addition to the culture media. G-hPRL was then purified and extensively characterized, comparing its bioactivity, clearance rate, N-glycan structures, monosaccharide composition and molecular mass to those of the native hormone. N-glycoprofiling, together with MALDI-TOF-MS molecular mass determination, proved to be extremely useful tools whose application can be readily extended to the glycan structure analysis and glycosylation site occupancy determination of polyglycosylated proteins. We emphasize that, when looking for the biological

activity or in vivo action of human glycosylated prolactin or of other glycoprotein hormones, especially when used as biopharmaceuticals, one must always consider that CHO-derived material is clearly not identical to the native, pituitary material.

Acknowledgements

The authors are grateful to José Maria de Sousa for valuable and skilled technical assistance. This work was supported by FAPESP, São Paulo, Brazil (Project 11/22985-3), by CAPES, Brasilia, by CNPq (Projects PQ 300473/2009-5, DT 310512/2010-7, and 479455/2011-2), Brasília, and by FK Biotecnologia/Proteogenética, Porto Alegre, RS, Brazil.

Appendix A. Supplementary data

Supplementary data associated with this article can be found, in the online version, at http://dx.doi.org/10.1016/j.jbiotec.2014.11.034.

References

Apweiler, R., Hermjakob, H., Sharon, N., 1999. On the frequency of protein glycosylation, as deduced from analysis of the SWISS-PROT database. Biochim. Biophys. Acta 1473, 4–8.

Arthuso, F.S., Bartolini, P., Soares, C.R., 2012. Laboratory production of human prolactin from CHO cells adapted to serum-free suspension culture. Appl. Biochem. Biotechnol. 167, 2212–2224.

Baenziger, J.U., 2003. Glycoprotein hormone GalNAc-4-sulphotransferase. Biochem. Soc. Trans. 31, 326–330.

Barone, R., Sturiale, L., Garozzo, D., 2009. Mass spectrometry in the characterization of human genetic N-glycosylation defects. Mass Spectrom. Rev. 28, 517–542.

Bernichtein, S., Touraine, P., Goffin, V., 2010. New concepts in prolactin biology. J. Endocrinol. 206, 1–11.

Dalmora, S., Oliveira, J.E., Affonso, R., Gimbo, E., Ribela, M.T., Bartolini, P., 1997. Analysis of recombinant human growth hormone directly in osmotic shock fluids. J. Chromatogr. A 782, 199–210.

Damiani, R., Almeida, B.E., Oliveira, J.E., Bartolini, P., Ribela, M.T., 2013. Enhancement of human thyrotropin synthesis by sodium butyrate addition to serum-free CHO cell culture. Appl. Biochem. Biotechnol. 171, 1658–1672.

Desaire, H., 2013. Glycopeptide analysis, recent developments and applications. Mol. Cell. Proteomics 12, 893–901.

Fernandez, I., Touraine, P., Goffin, V., 2010. Prolactin and human tumourigenesis. J. Neuroendocrinol. 22, 771–777.

Fideleff, H.L., Sequera, A.M., Ruibal, G.F., Boquete, H.R., Suarez, M.G., Colombani, M., Azaretzky, M., Brunetto, O., Scaglia, H.E., 2012. Cosecretion of glycosylated prolactin and non-glycosylated prolactin from childhood to the end of puberty. Horm. Res. Paediatr. 77, 229–234.

Fogli, A., Merle, C., Roussel, V., Schiffmann, R., Ughetto, S., Theisen, M., Boespflug-Tanguy, O., 2012. CSF N-glycan profiles to investigate biomarkers in brain developmental disorders: application to leukodystrophies related to eIF2B mutations. PLoS ONE 7, e42688.

Freeman, M.E., Kanyicska, B., Lerant, A., Nagy, G., 2000. Prolactin: structure, function, and regulation of secretion. Physiol. Rev. 80, 1523–1631.

Gettler, L.T., McDade, T.W., Feranil, A.B., Kuzawa, C.W., 2012. Prolactin, fatherhood, and reproductive behavior in human males. Am. J. Phys. Anthropol. 148, 362–370.

Glezer, A., Soares, C.R., Vieira, J.G., Giannella-Neto, D., Ribela, M.T., Goffin, V., Bronstein, M.D., 2006. Human macroprolactin displays low biological activity via its homologous receptor in a new sensitive bioassay. J. Clin. Endocrinol. Metab. 91, 1048–1055.

Goffin, V., Binart, N., Touraine, P., Kelly, P.A., 2002. Prolactin: the new biology of an old hormone. Annu. Rev. Physiol. 64, 47–67.

Heller, S.R., Rodrigues Goulart, H., Arthuso, F.S., Oliveira, T.L., Bartolini, P., Soares, C.R., 2010. Synthesis, purification and characterization of recombinant glycosylated human prolactin (G-hPRL) secreted by cycloheximide-treated CHO cells. J. Biotechnol. 145, 334–340.

Laemmli, U.K., 1970. Cleavage of structural proteins during the assembly of the head of bacteriophage T4. Nature 227, 680–685.

Lehr, T., Geyer, H., Maab, K., Doenhoff, M.J., Geyer, R., 2006. Structural characterization of N-glycans from the freshwater snail Biomphalaria glabrata cross-reacting with *Schistosoma mansoni* glycoconjugates. Glycobiology 17, 82–103.

Lin, C.Y., Ma, Y.C., Pai, P.J., Her, G.R., 2012. A comparative study of glycoprotein concentration, glycoform profile and glycosylation site occupancy using isotope labeling and electrospray linear ion trap mass spectrometry. Anal. Chim. Acta 728, 49–56.

Losfeld, M.E., Soncin, F., Ng, B.G., Singec, I., Freeze, H.H., 2012. A sensitive green fluorescent protein biomarker of N-glycosylation site occupancy. FASEB J. 26, 4210–4217.

Mi, Y., Fiete, D., Baenziger, J.U., 2008. Ablation of GalNAc-4-sulfotransferase-1 enhances reproduction by altering the carbohydrate structures of luteinizing hormone in mice. J. Clin. Invest. 118, 1815–1824.

Hashii, N., Kawasaki, N., Itoh, S., Harazono, A., Matsuishi, Y., Hayakawa, T., Kawanishi, T., 2005. Specific detection of Lewis x-carbohydrates in biological samples using liquid chromatography/multiple-stage tandem mass spectrometry. Rapid Commun. Mass Spectrom. 19, 3315–3321.

Pan, S., Tamura, Y., Chen, R., May, D., McIntosh, M.W., Brentnall, T.A., 2012. Large-scale quantitative glycoproteomics analysis of site-specific glycosylation occupancy. Mol. Biosyst. 8, 2850–2856.

Petrescu, A.J., Milac, A.L., Petrescu, S.M., Dwek, R.A., Wormald, M.R., 2004. Statistical analysis of the protein environment of N-glycosylation sites: implications for occupancy, structure, and folding. Glycobiology 14, 103–114.

Price, A.E., Logvinenko, K.B., Higgins, E.A., Cole, E.S., Richards, S.M., 1995. Studies on the microheterogeneity and in vitro activity of glycosylated and nonglycosylated recombinant human prolactin separated using a novel purification process. Endocrinology 136, 4827–4833.

Rafferty, B., Rigsby, P., Gaines-Das, R.E., 2001. Draft Report of an International Collaborative Study of the Proposed WHO Reference Reagents for rDNA-derived Prolactin and Its Glycosylated and Non-glycosylated Components. WHO, Geneva, Switzerland.

Shelikoff, M., Sinskey, A.J., Stephanopoulos, G., 1994. The effect of protein synthesis inhibitors on the glycosylation site occupancy of recombinant human prolactin. Cytotechnology 15, 195–208.

Sinha, Y.N., 1995. Structural variants of prolactin: occurrence and physiological significance. Endocr. Rev. 16, 354–369.

Soares, C.R., Camargo, I.M., Morganti, L., Gimbo, E., Oliveira, J.E., Legoux, R., Ferrara, P., Bartolini, P., 2002. Reversed-phase high-performance liquid chromatography method for the determination of prolactin in bacterial extracts and in its purified form. J. Chromatogr. A 955, 229–236.

Soares, C.R., Glezer, A., Okazaki, K., Ueda, E.K., Heller, S.R., Walker, A.M., Goffin, V., Bartolini, P., 2006. Physico-chemical and biological characterizations of two human prolactin analogs exhibiting controversial bioactivity, synthesized in Chinese hamster ovary (CHO) cells. Protein Expr. Purif. 48, 182–194.

Soares, C.R., Morganti, L., Miloux, B., Lupker, J.H., Ferrara, P., Bartolini, P., 2000. High-level synthesis of human prolactin in Chinese-hamster ovary cells. Biotechnol. Appl. Biochem. 32 (Pt 2), 127–135.

Soares, C.R., Ueda, E.K., Oliveira, T.L., Gomide, F.I., Heller, S.R., Bartolini, P., 2008. Distinct human prolactin (hPRL) and growth hormone (hGH) behavior under bacteriophage lambda PL promoter control: temperature plays a major role in protein yields. J. Biotechnol. 133, 27–35.

Suzuki, M.F., Arthuso, F.S., Oliveira, J.E., Oliveira, N.A., Goulart, H.R., Capone, M.V., Ribela, M.T., Bartolini, P., Soares, C.R., 2012. Expression, purification, and characterization of authentic mouse prolactin obtained in *Escherichia coli* periplasmic space. Biotechnol. Appl. Biochem. 59, 178–185.

Tian, Y., Zhang, H., 2010. Glycoproteomics and clinical applications. Proteomics Clin. Appl. 4, 124–132.

Tworoger, S.S., Eliassen, A.H., Rosner, B., Sluss, P., Hankinson, S.E., 2004. Plasma prolactin concentrations and risk of postmenopausal breast cancer. Cancer Res. 64, 6814–6819.

Wu, W., Coss, D., Lorenson, M.Y., Kuo, C.B., Xu, X., Walker, A.M., 2003. Different biological effects of unmodified prolactin and a molecular mimic of phosphorylated prolactin involve different signaling pathways. Biochemistry 42, 7561–7570.

Yu, S.Y., Wu, S.W., Hsiao, H.H., Khoo, K.H., 2009. Enabling techniques and strategic workflow for sulfoglycomics based on mass spectrometry mapping and sequencing of permethylated sulfated glycans. Glycobiology 19, 1136–1149.